第31卷第4期
2012年8月

红外与毫米波学报
J. Infrared Millim. Waves

Vol. 31, No. 4
August, 2012

文章编号:1001-9014(2012)04-0289-05

DOI:10.3724/SP.J.1010.2012.00289

Microstructures and optical properties of relaxor ferroelectric 0.74Pb($Mg_{1/3}Nb_{2/3}$)O_3-0.26$PbTiO_3$ thin films

TIAN Yue[1], TANG Yan-Xue[1]*, ZHOU Dan[1], HU Zhi-Juan[1],
WANG Fei-Fei[1], CHEN Xin-Man[1], LIU Feng[1], WANG Tao[1], XIE Dong-Zhu[1],
SUN Da-Zhi[1], SHI Wang-Zhou[1], HU Gu-Jin[2], KONG Wei- Jin[3]

(1. Key Laboratory of Optoelectronic Material and Device, Shanghai Normal University, Shanghai 200234, China;
2. National Laboratory for Infrared Physics, Shanghai Institute of Technical Physics,
Chinese Academy of Sciences, Shanghai 200083, China;
3. College of Physics Science, Qingdao University, Qingdao 266071, China)

Abstract: Relaxor ferroelectric 0.74Pb($Mg_{1/3}Nb_{2/3}$)O_3-0.26$PbTiO_3$ thin films were prepared on $LaNiO_3$-buffered silicon substrates by radio-frequency magnetron sputtering. The effect of deposition temperature on films' microstructures and optical properties was investigated. The sample deposited at 500 °C exhibits not only a pure perovskite phase, highly (110)-preferred orientation, and dense and crack-free morphology, but also the largest average remnant polarization of 17.2 μC/cm^2 among all investigated films. With Cauchy model the refractive indices and extinction coefficients for these specimens have been obtained by fitting experimental reflectance spectra. At a wavelength of 633 nm, the value of refractive index 2.41 was obtained for the thin films deposited at 500 °C. In addition, optical band gaps of the films are in the range of 2.97-3.22 eV. A preliminary discussion has been carried out on the difference in the optical properties of these films.

Key words: PMN-0.26PT ferroelectric thin films; refractive indices; extinction coefficients
PACS: 78.20.Ci, 77.84.-s, 77.84.Dy

弛豫铁电0.74Pb($Mg_{1/3}Nb_{2/3}$)O_3-0.26$PbTiO_3$薄膜的微结构和光学性能

田 玥[1], 唐艳学[1]*, 周 丹[1], 胡志娟[1], 王飞飞[1], 陈心满[1],
刘 锋[1], 王 涛[1], 谢东珠[1], 孙大志[1], 石旺舟[1], 胡古今[2], 孔伟金[3]

(1. 上海师范大学 光电材料与器件重点实验室, 上海 200234;
2. 中国科学院上海技术物理研究所 红外物理国家重点实验室, 上海 200083;
3. 青岛大学 物理科学学院, 山东 青岛 266071)

摘要: 采用磁控溅射法, 选用$LaNiO_3$作为缓冲层, 在硅基片上制备出了0.74Pb($Mg_{1/3}Nb_{2/3}$)O_3-0.26$PbTiO_3$弛豫铁电薄膜. 研究了沉积温度对薄膜的微结构和光学性能的影响. 其中, 沉积温度为500 °C时制备的薄膜, 不仅具有纯的钙钛矿结构, 高度(110)择优取向、致密、无裂纹的形貌, 而且具有最大的剩余极化, 大小为17.2 μC/cm^2. 使用柯西模型进行拟合反射谱, 分析得到薄膜的折射率和消光系数. 在波长为633 nm时, 500 °C沉积的薄膜的折射率大小为2.41. 另外, 薄膜的光学带隙在2.97~3.22 eV范围内. 并初步讨论了这些薄膜的光学性能的差异.

关 键 词: PMN-0.26PT铁电薄膜; 折射率; 消光系数
中图分类号: O469 **文献标识码**: A

Received date: 2011-04-30, **revised date**: 2012-03-10 **收稿日期**: 2011-04-30, **修回日期**: 2012-03-10
Foundation items: Supported by National Natural Science Foundation of China (60807036, 10774154, 11074265, 10804060), the "Chenguang" Program of Shanghai Educational Development Foundation of China (2007CG57), the Science and Technology Commission of Shanghai Municipality (10ZR1422300), and Shanghai Municipal Education Commission (11YZ83).
Biography: TIAN Yue (1985-), male, Shenyang, China, Bachelor. Research area involves preparation and properties of ferroelectric thin films.
* **Corresponding author**: E-mail: yanxuetang@yahoo.com.cn.

Introduction

Recent years, relaxor ferroelectric $(1-x)$ Pb $(Mg_{1/3}Nb_{2/3})O_3$-$xPbTiO_3$ (PMN-PT) single crystals have attracted much attention due to their excellent dielectric, ferroelectric, piezoelectric, pyroelectric, and electro-optical properties[1-4]. They are good candidates for various applications, for example nonvolatile memories, actuators, transducers, infrared detectors, and nonlinear photonic devices[1-6]. Many techniques such as sol-gel, metal organic chemical vapor deposition, radio-frequency (RF) magnetron sputtering, and pulsed laser deposition, etc., were used to grow PMN-PT thin films at high temperatures (575 ~ 850°C)[7-10]. However, with the miniaturization of photoelectronic devices, it is desirable to fabricate high-quality thin films on silicon substrates at lower temperatures[11-12].

In the past two decades, many studies had been done on PMN-PT thin films' ferroelectric, dielectric, and electromechanical performance[7-10]. There are a lot of reports on the optical parameters of PMN-PT single crystals and $PbTiO_3$ ceramics, but literatures on the optical information of PMN-PT thin films are relatively scare[3-4]. It is interesting to note that $(1-x)$ PMN-xPT single crystals with $x=0.26$, beyond morphotropic phase boundary (MPB) ($0.30 < x < 0.35$), show excellent ferroelectric and optical properties, as well as stably properties due to higher depolarization temperature[2,4]. In this paper, we explore the effect of deposition temperature on the microstructures and optical properties of the PMN-0.26PT thin films deposited by radio-frequency (RF) magnetron sputtering.

1 Experimental procedure

PMN-0.26PT powder was synthesized firstly by sintering the blend of Nb_2O_5, MgO, PbO, and TiO_2 starting materials. To compensate for the loss of Pb and Mg during high temperature treatment, the blend has an excess of 10 mol% PbO and 5 mol% MgO, respectively. The resultant powder was compressed into a plate with a diameter of ~2 inch and a thickness of ~3 mm. The synthesized target was then sintered at 1200 °C for 2 h.

Conductive and pseudo-cubic $LaNiO_3$ (LNO) thin film was selected as the interlayer between PMN-0.26PT thin film and silicon wafer, because it exhibits a good flexibility and a lattice constant of 0.384 nm matching wen with most of the perovskite ferroelectric oxides[2]. The LNO-coated Si wafers were heated by a halogen lamp up to the temperature desired in vacuum chamber. The background pressure was kept at 1.5×10^{-5} Pa and the processing conditions for growth of PMN-0.26PT thin films were listed in Table 1.

Table 1 Processing conditions for fabricating PMN-0.26PT thin films

表1 PMN-0.26PT 薄膜的制备条件

Target composition	PMN-0.26PT
Target diameter	Φ2 inch
Target-substrate distance	9 cm
RF power	150 W
Gas ratio	Ar: O_2 = 36:4
Sputtering pressure	2 pa
Substrate	LNO/(100)Si
Substrate temperature	From 200 to 650 °C

The crystallographic quality and microstructure of PMN-0.26PT thin films were characterized by X-ray diffraction (XRD) spectrometer with Cu Kα radiation source (Model D/Max-rA, Rigaku, Tokyo, Japan) and field emission scanning electron microscopy (FESEM, Siron200 1615, FEI Company, Hillsboro, OR). The ferroelectric properties of the films were analyzed by using a RT66A ferroelectric test system (Radiant Technologies, Albuquerque, NM). The reflectance spectra of the samples were measured at room temperature (RT) by a Perkin Elmer Lambda 800/900 UV/visible spectrometer with incident light perpendicular to the sample's surface. As determined by cross-sectional SEM image and standard four-probe technique, the thickness and room temperature (RT) resistivity of LNO film are ~100 nm and 7×10^{-4} Ω · cm, respectively.

2 Results and discussion

2.1 Microstructures

Fig. 1 represents the XRD patterns for the PMN-0.26PT thin films deposited in the temperature range of 200-650 °C. All the films deposited below 500 °C are in amorphous state, while those films grown in the temperature region 500-600 °C show highly (110)-preferred orientation and single perovskite phase. For the films grown at temperatures higher than 600 °C, pyrochlore phases appear because of volatilization of PbO.

As shown in Fig. 2, these PMN-0.26PT thin films deposited at 500 °C, 550 °C, and 600 °C (de-

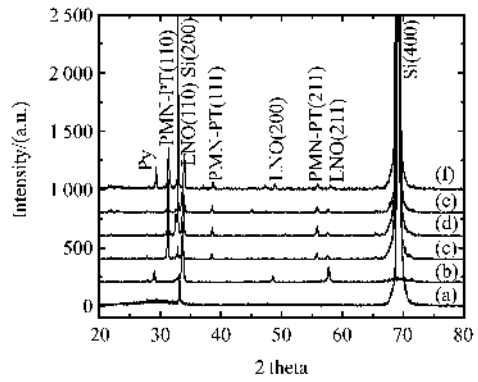

Fig. 1 X-ray diffraction patterns for the PMN-0.26PT thin films deposited at (a) 200 °C, (b) 450 °C, (c) 500 °C, (d) 550 °C, (e) 600 °C, and (f) 650 °C. The pyrochlore phase is labeled as Py
图1 不同温度下沉积的 PMN-0.26PT 薄膜的 X 射线衍射图谱 (a) 200 °C, (b) 450 °C, (c) 500 °C, (d) 550 °C, (e) 600 °C, (f) 650 °C. 焦绿石相以 Py 表示

noted as samples A, B, and C, respectively) exhibit dense and crack-free surface morphologies and comprise of well distinguishable grains. The sample A is composed of small uniform grains with size in the range of 50 ~ 150 nm. With deposition temperature increasing, the grain size becomes larger gradually. The thicknesses of samples A, B, and C are 650 nm, 630 nm, and 600 nm, respectively, determined from the cross-sectional SEM photographs (not shown). The thickness of PMN-0.26PT films decreases with deposition temperature increasing owing to the densification.

Generally, the lowest growth temperature ~ 580 °C is required to acquire high quality $(1-x)Pb(Mg_{1/3}Nb_{2/3})O_3$-$xPbTiO_3$ films [7-10]. In the present work, the crystallization temperature of 500 °C enable the PMN-0.26PT thin films to be converted into a rhombohedral phase, implying that the process is compatible with the existing Si-based integrated circuit technology.

2.2 Electric properties

Fig. 3 plots the RT polarization-electric field (P-E) characteristic curves for samples A, B, and C under the maximum polarization voltage of 25 V. The driving voltage is a single bipolar triangular wave with a frequency of 50 Hz. Each specimen shows a well-defined hysteresis loop. The average remnant polarization P_r is in the range of 8.1 ~ 17.2 μC/cm^2, and the coercive field E_c varies in the region of 76.2 ~ 106.1 kV/cm. Sample A has a largest value of P_r ~

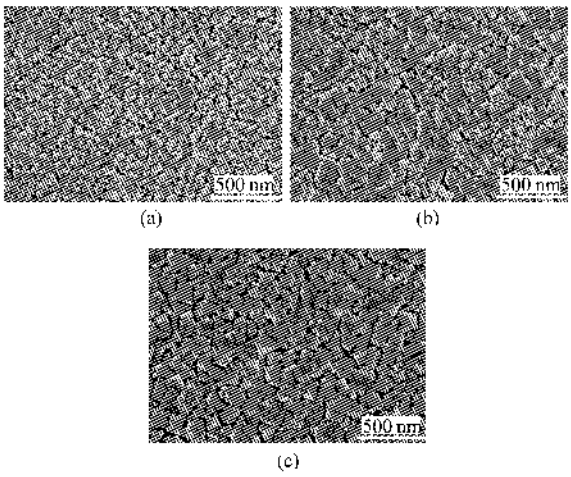

Fig. 2 Surface SEM images for samples A, B, and C
图2 样品 A,B,C 的 SEM 图谱

17.2 μC/cm^2. To check the effect of the leakage current I_L on the P_r, we performed a leakage current measurement on each thin film capacitor with an area of 0.5 × 0.5 mm^2. Under a DC voltage of 25 V, the measured maximum of the I_L is 3.5 × 10^{-7} A. Based on the above results, the largest contribution to the P_r aroused by the I_L is calculated to be 0.7 μC/cm^2, which is much smaller than the experimental value of the P_r, suggesting that the P_r in the PMN-0.26PT thin films mainly comes from their intrinsic electric polarization.

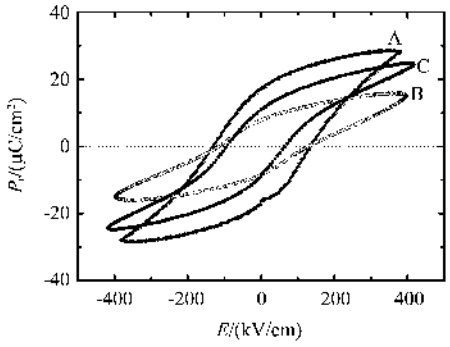

Fig. 3 Ferroelectric hysteresis loops for samples A, B, and C. The data were taken at the maximum driving voltage of 25 V
图3 样品 A,B,C 的电滞回线. 测试时施加的最大电压是 25V

2.3 Optical properties

The optical properties of PMN-0.26PT films were analyzed according to the method reported in the literature[13]. The optical constants of LNO electrode were extracted with Drude-Lorentz model, and the

PMN-0.26PT films were extracted with Cauchy model, where the complex refractive index of single silicon was treated as known quantity. Figure 4 depicts the optical reflectance spectra for the PMN-0.26PT/LNO/Si system. In the examined frequency region, since the 100 nm LNO layer has a strong absorption and is nearly opaque to light[13], the observed stripes originate primarily from the interference of the light being reflected at the top surface and the PMN-0.26PT/LNO interface. The solid lines in Fig. 4 represent the simulations to the PMN-0.26PT/LNO multilayers, rendering a relative coincidence between the experimental and theoretical results but a significant deviation below 600 nm wavelengths. This deviation may be originated from the random scattering of light by the rough surface and grains with a size comparable to the wavelengths of the incident light.

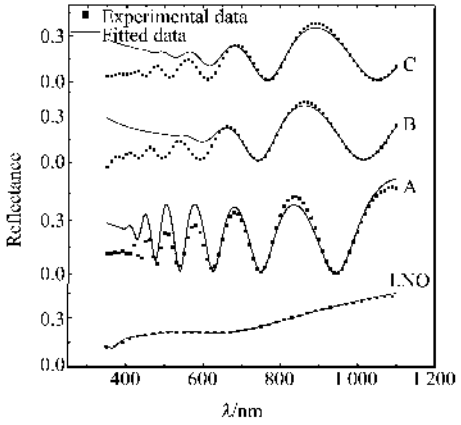

Fig. 4 Optical reflectance spectra for LNO layer and samples A, B, and C
图4 LNO层和样品A,B,C的光学反射谱

Fig. 5 shows the effective refractive indices n and extinction coefficients k for the LNO and the PMN-0.26PT thin films. As can be seen, both n and k of the films decrease with wavelength increasing. In the weak absorption region, the value of n for the thin films deposited at 500 °C is larger than that of films deposited at other temperatures, which may be attributed to the more homogeneous thin film structure. From Figs. 1 and 2, it can be found, that the samples B and C have similar crystallinity and topography, resulting in a similar optical property. On the other hand, at wavelength over 500 nm, the k values for these samples get nearly coincident and smaller than 0.1, indicating that the PMN-0.26PT thin films become transparent in this wavelength region. As to the reasons for the discrepancy in k values at high frequency region (> 10^{14} Hz), it is still unclear at present.

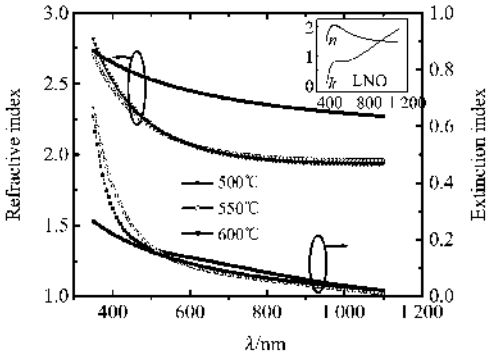

Fig. 5 Wavelength dependence of refractive indices and extinction coefficients for samples A, B, and C at room temperature. The inset is wavelength dependence of refractive indices and extinction coefficients for LNO thin films
图5 室温下样品A,B,C的折射率和消光系数随着波长的变化.图5中的图是LNO薄膜的折射率和消光系数随着波长的变化

Optical loss of a dielectric medium comes principally from the absorption without consideration of scattering and reflection. Since PMN-PT is a direct band-gap material and the interband transition excitation is the most predominated absorption, equation (1) can be used to estimate its optical band-gap[14]

$$\alpha E = C_d (E - E_g^d)^{1/2}, \quad (1)$$

where α is the absorption coefficient of PMN-PT associated with k in the form $\alpha = 4\pi\kappa/\lambda$, E is the photon energy, and C_d is a constant. As shown in Fig. 6, near the absorption edge $(\alpha E)^2$ varies linearly with E. In other words, the absorption coefficient and the photon energy of the PMN-PT thin films satisfy Eq. (1) simultaneously. By extrapolating the linear portion of the plot to $(\alpha E)^2 = 0$ in Fig. 6, the estimated values of E_g^d are 3.22, 3.17, and 2.97 eV for samples A, B, and C, respectively. E_g^d of the PMN-PT film decreases with deposition temperature increasing in the investigated temperature range. The shift of band-gap energy was mainly due to both the crystallinity and defect in the PMN-PT thin films[13]. As the substrate temperature increased to 600 °C, the thin films show larger and non-uniform grain size as shown in Fig. 2. In addition, Pb vacancies occur due to volatilization of PbO at higher temperature, which contributes to the lowest energy bands.

3 Conclusions

In summary, pure perovskite and (110)-pre-

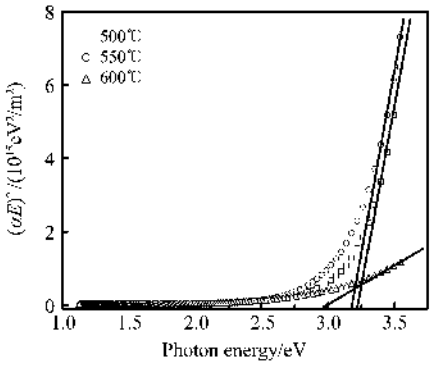

Fig. 6 $(\alpha E)^2$ vs. E curves for samples A, B, and C at room temperature
图6 室温下样品A,B,C的$(\alpha E)^2$随着光子能量E的变化

ferred oriented PMN-0.26PT thin films have been fabricated on LNO/Si substrates at relatively lower temperatures. Deposition temperature has a significant effect on crystalline structure, surface morphology, together with ferroelectric and optical properties of PMN-0.26PT films. All PMN-0.26PT films grown in the temperature range of 500-600 °C possess good ferroelectricity. At the wavelength of 633 nm, the value of refractive index is ~ 2.41 for the PMN-0.26PT thin film deposited at 500 °C, which is in agreement with that reported. The optical band-gaps of the PMN-PT thin films vary in the range of 2.97 ~ 3.22 eV.

REFERENCES

[1] Fu H, Cohen R E. Polarization rotation mechanism for ultrahigh electromechanical response in single-crystal piezoelectrics [J]. *Nature*, 2000, **403**: 281 - 283.

[2] Tang Y X, Wan X M, Zhao X Y, *et al*. Large pyroelectric response in relaxor-based ferroelectric (1-x)Pb($Mg_{1/3}Nb_{2/3}$)O_3-$x$$PbTiO_3$ single crystals [J]. *J. Appl. Phys.*, 2005, **98**(8): 084104.

[3] Wan X M, Xu H Q, He T H, *et al*. Optical properties of tetragonal Pb($Mg_{1/3}Nb_{2/3}$)$_{0.62}Ti_{0.38}O_3$ single crystal [J]. *J. Appl. Phys.*, 2003, **93**(8): 4766 - 4768.

[4] Wan X M, Chan H L W, Choy C L, *et al*. Optical properties of (1-x)Pb($Mg_{1/3}Nb_{2/3}$)O_3-$x$$PbTiO_3$ single crystals studied by spectroscopic ellipsometry [J]. *J. Appl. Phys.*, 2004, **96**(3): 1387 - 1391.

[5] Segal M. Ferroelectric memory: slim fast [J]. *Nat. Nanotechnol.*, 2009, 4(7): 405.

[6] Sekitani T, Yokota T, Zschieschang U, *et al*. Organic nonvolatile memory transistors for flexible sensor arrays [J]. *Science*, 2009, **326**(5959): 1516 - 1519.

[7] Fan H, Kim H. Microstructure and electrical properties of sol-gel derived Pb($Mg_{1/3}Nb_{2/3}$)$_{0.7}Ti_{0.3}O_3$ thin films with single perovskite phase [J]. *Jpn. J. Appl. Phys.*, 2002, **41**(11B): 6768 - 6772.

[8] Yokoyama S, Okamoto S, Funakubo H, *et al*. Crystal structure, electrical properties, and mechanical response of (100)-/(001)-oriented epitaxial Pb($Mg_{1/3}Nb_{2/3}$)O_3-PbTiO_3 films grown on (100)c$SrRuO_3$ | | (100) $SrTiO_3$ substrates by metal-organic chemical vapor deposition [J]. *J. Appl. Phys.*, 2006, **100**(5): 054110.

[9] Donnelly N J, Catalan G, Morros C, *et al*. Dielectric and electromechanical properties of Pb($Mg_{1/3}$, $Nb_{2/3}$)O_3-PbTiO_3 thin films grown by pulsed laser deposition [J]. *J. Appl. Phys.*, 2003, **93**(12): 9924 - 9929.

[10] Tsang W S, Chan K Y, Mark C L, *et al*. Spectroscopic ellipsometry study of epitaxially grown Pb($Mg_{1/3}Nb_{2/3}$)O_3-$PbTiO_3$/MgO/TiN/Si heterostructures [J]. *Appl. Phys. Lett.*, 2003, **83**(8): 1599 - 1601.

[11] Mischenko A S, Zhang Q, Scott J F, *et al*. Giant electrocaloric effect in thin-film $PbZr_{0.95}Ti_{0.05}O_3$ [J]. *Science*, 2006, **311**(5765): 1270 - 1271.

[12] Tantigate C, Lee J, Safan A. Processing and properties of Pb($Mg_{1/3}Nb_{2/3}$)O_3-$PbTiO_3$ thin films by pulsed laser deposition [J]. *Appl. Phys. Lett.*, 1995, **66**(3): 1611 - 1613.

[13] Bao D H, Yao X, Shinozaki K, *et al*. Crystallization and optical properties of sol-gel-derived PbTiO3 thin films [J]. *J. Phys. D: Appl. Phys.*, 2003, **36**(17): 2141 - 2145.

[14] DrDomenico M, Jr. Wemple S H. Oxygen-octahedra ferroelectrics. I. theory of electro-optical and nonlinear optical effects [J]. *J. Appl. Phys.*, 1969, **40**(2): 720 - 734.